Deformation Behaviour of Soils in Terms of Soil Moduli

The Third Laurits Bjerrum Memorial Lecture
Presented 27th February, 1978

By Oddvin Tokheim

INTRODUCTION

The Mohr-Coulomb failure criterion for soils is credited to Coulomb more than two hundred years ago. Nevertheless, it seems fair to say that soil mechanics as science was founded not more than 60 years ago owing to the remarkable work by Terzaghi through the years 1919–25 (Ref. 31). He defined the effective stress principle and spelled out the consolidation theory for soils.

In the early days of the soil mechanics history, the science of solid materials had already existed for a long time. Soil mechanics developed along with the need for solving engineering problems. It comes as no surprise that existing theories regarding failure and deformations to a large extent were adopted and applied to soils without a rigorous examination of their validity. A major obstacle to such confirmation has been the lack of adequate testing equipment and experimental methods.

Over the last decade or two extensive research has dwelt into pre- and post-failure behaviour of soils, including evaluation of failure criteria. Høeg (1978) has done a recent review of this development in the Second Laurits Bjerrum Memorial Lecture.

Furthermore, a number of papers representing fairly well the state-of-the-art were presented in a specialty session at the Ninth ICSMFE in Tokyo (Ref. 13).

This Lecture does not aim to review the different approaches to modelling of soil deformation behaviour; rather certain aspects of soil behaviour will be looked into along with the presentation of a new stress-strain model. This model was developed by the lecturer as part of a doctorate study at the Norwegian Institute of Technology (32). A few more lines shall however first be reserved to look into the recent trends in soil modelling.

After the mid-sixties several attempts (6, 9, 10) have been made to modify isotropic, linear-elastic theory to account for the non-linear nature of soil behaviour. Together with the computer technique becoming available, a large step was taken towards more realistic solutions to complicated soil deformation problems. However, there is some concern (21) about formal questions involved in some of the simple modified elastic models which are meant to account for non-linearity. Experimental results have also indicated that the plastic nature of soils may not be readily represented by simple elastic models.

Drucker and Prager (7, 8) first applied plasticity theory to limit analysis of soil problems in the early 1950's. However, plasticity theory was first used a decade later in the pioneering work at Cambridge University (25, 26, 27) to tailor a stress-strain theory for soils.

The 'Cambridge Model' was developed before powerful numerical techniques became available. These techniques greatly advanced in the mid seventies and allowed the implementation of various elasto-plastic stress-strain models in finite element programs (34).

The most recent half-decade has seen a trend into elasto-plastic modelling of soils on the formal grounds of plasticity theory (19, 23). These models emphasize describing yielding in a way consistent with that of soil. A model by Prévost and Høeg (1977) also offers the possibility of dealing with inherent anisotropy of natural soils.

The model to be presented attempts to describe in a straightforward manner soil behaviour as observed in triaxial tests. Including also some basic principles of plasticity theory, a complete three-dimensional model is formulated. Strictly, the model may be classified as neither elasticity theory, nor plasticity theory.

However, we shall first look into some of the basic factors governing soil behaviour.

FACTORS AFFECTING SOIL BEHAVIOUR

Such factors may conveniently be divided into two groups. On one hand come properties and characteristics essentially inherited from the formation of a deposit, such as (mineral) composition, grain size, shape and distribution, and the nature of the pore fluid. In order to learn *why* soil behaves in a specific manner it is necessary to look into the fabric.

On the other hand come the state variables: load (stress), deformation (strain), time and temperature.

Most research work has been devoted to interrelations between the state variables, as will this lecture.

In the following, we shall be basically concerned with a relation between stress and strain histories or stress and strain paths. Time effects like creep will be ignored and isothermal conditions will be considered.

THE EFFECTIVE STRESS PRINCIPLE

Terzaghi (1936) stated the effective stress principle (ESP) explicitly as follows:

> All the measureable effects of a change of the stress, such as compression, distortion and a change of the shearing resistance are *exclusively* due to changes in the effective stresses.

Although very simple and having met with virtually no argument about its validity, the principle has not been fully understood and appreciated until quite recently.

The ESP implies *a unique relation between strain history and effective stress history.*

For a time-independent material, i.e. no deformation may take place under constant effective stress, the ESP may be rephrased into: *there is a unique relation between a strain path and an effective stress path.*

It is emphasized that the ESP does not imply a unique relation between strain and effective stress. The state of strain depends not only on the effective stress, but also on the effective stress history.

In order to demonstrate the validity of the ESP, we shall see that it applies to loading in a triaxial cell. Assume that loading takes place under constant volume (CV). Under such conditions, only two strain paths or strain systems are possible; namely axial compression and axial extension. Hence only two effective stress paths should be available for a time-independent material. Any total stress path causing compression should imply a unique effective stress path for given initial stresses. The same goes for extension.

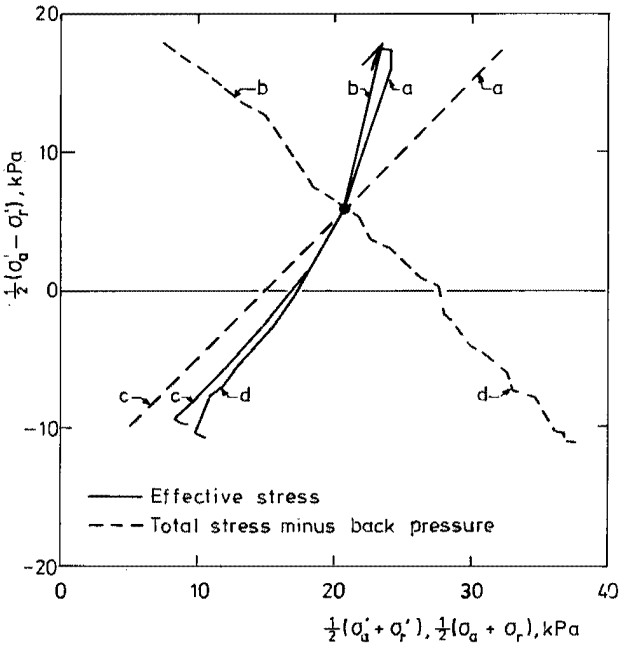

Fig. 1. Effective and total stress paths of undrained triaxial compression and extension tests. After Bishop and Wesley (1975).

Figure 1 shows results of undrained triaxial compression and extension tests run by Bishop and Wesley (1975) on saturated clay. As seen, widely different total stress paths result in virtually the same effective stress path. The slight lack of coincidence between the effective stress paths is probably due to a small volume change during undrained shear.

Plane strain extension and compression tests (5) have also shown that effective stress-strain plots are virtually unaffected by the total stresses.

The model presented herein relates paths of effective stresses to strain paths, hence implying the ESP.

STRENGTH OF SOILS

This lecturer has never seen a precise and thorough definition of failure applying to all soils. The problem of definition is associated with the variety of ways in which failure may take place. Some soils behave in a brittle manner, while others yield over a considerable stress range. The nature of the failure may as well depend on the actual stress level applied to the soil.

From an engineering point of view, failure should preferably be defined in terms of deformation or at least be related to deformation. In Norway it is becoming increasingly common to define a characteristic strength at strains of the order of 2%, although the ultimate failure likely takes place at strains of the order of 10%. Figure 2 presents typical effective stress paths of an overconsolidated clay.

The Mohr-Coulomb failure criterion, generally accepted as a reasonably accurate failure criterion for most soils, does not include the intermediate principal stress. Figures 3 and 4 illustrate the Mohr-Coulomb failure criterion. However, as true (cubical) triaxial apparatuses and other elaborate testing equipments have been developed, the significance of the intermediate principal stress has been investigated.

Tests run so far on various sands (11, 16, 18, 29) and on remoulded clay (28) have on the whole led to the following conclusion: The appearant Mohr-Coulomb friction angle φ as determined from various tests in which σ_2' is greater than σ_3', tends to be moderately higher than the corresponding φ-value from triaxial compression tests ($\sigma_2' = \sigma_3'$); σ_2' and σ_3' denoting the intermediate and the minor principal effective stress respectively.

Tests on cemented clay (33) have, however, indicated that inherent anisotropy due to sedimentation and aging under anisotropic stress conditions may be far more important than the relative magnitude of σ_2'. No rigorous failure criterion known to this lecturer is however capable of handling inherent anisotropy.

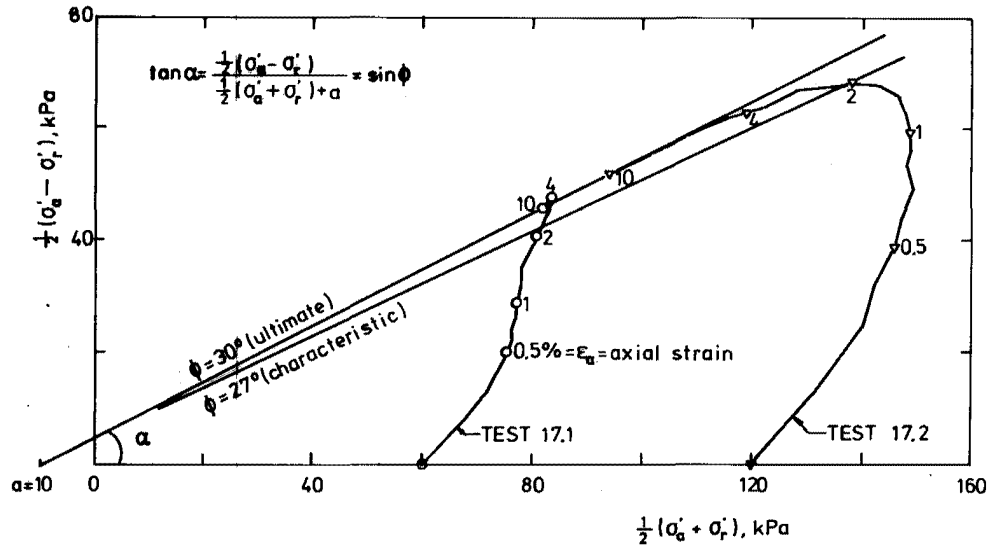

Fig. 2. Undrained triaxial compression tests on overconsolidated clay from Åndalsnes (by Kummeneje, Trondheim).

The effective stress principle (ESP) suggests that shear strength should be defined in terms of effective stresses. Nevertheless, undrained shear strength in terms of total stresses still represents the most common strength criterion for clay. At first thought this may seem to contradict the ESP. However, undrained shearing represents a particular deformation pattern or strain history to which, according to the ESP, a particular stress path or stress history corresponds. Once the stress path is given, the *failure shear stress* or undrained shear strength is defined as well. For instance, in Fig. 2 the undrained shear strength in triaxial compression is the maximum shear stress appearing at the peak of the stress path. Thus there is no contradiction between the ESP and the notion of undrained shear strength. Rather the undrained shear strength is an implication of the ESP.

Figure 2 also demonstrates the lack of uniqueness of the undrained shear strength as two stress paths starting from different initial stresses indicate widely different strength values. This points out that the undrained strength is intimately related to stress history, including the initial effective stresses. Thus it is perhaps more adequate to use terms like *failure shear stress* under such and such conditions, rather than *undrained shear strength* which misleadingly indicates a physical constant or fundamental property of the soil. Due to recognition of the ESP, confidence in the undrained shear strength as determined from index tests like unconfined compression and fall cone tests is declining. More advanced methods like the ADP-analysis developed at NGI (1, 2, 4) and the SHANSEP-method (17) developed at MIT, combine the simplicity of undrained shear strength with the fundamentals of the ESP, also recognizing the importance of strength anisotropy.

As a conclusion of this section, failure of soils are governed by effective stresses in agreement with the ESP. Ignoring inherent anisotropy, the Mohr-Coulomb fail-

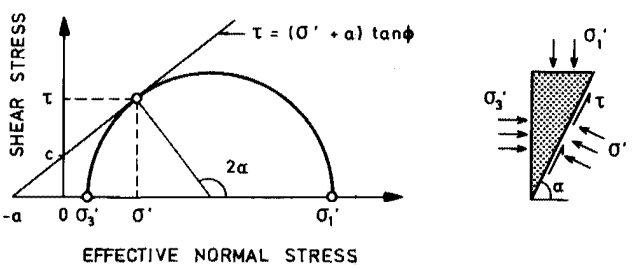

Fig. 3. The Mohr-Coulomb failure criterion.

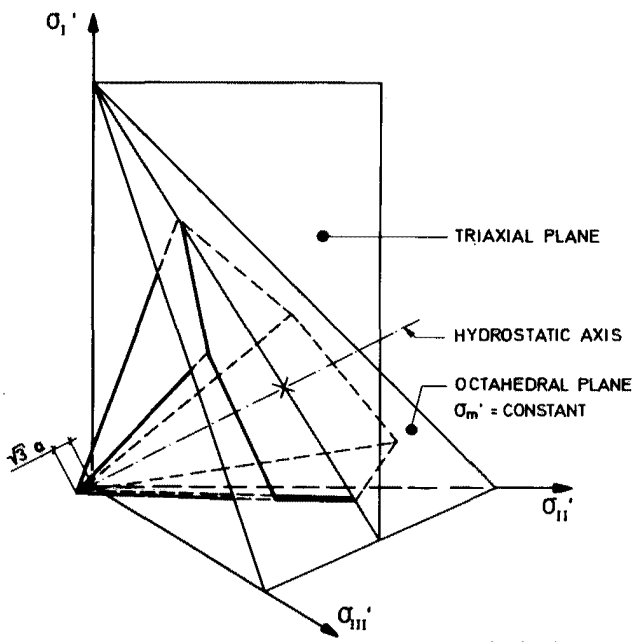

Fig. 4. Mohr-Coulomb failure surface in the principal stress space.

ure criterion is still considered to apply reasonably well to soils. The Mohr-Coulomb criterion is a corner-stone in the model presented herein.

COMMON ASPECTS OF SOIL COMPRESSION AND SHEARING

A variety of field and laboratory tests are available to explore the nature of soil deformation. The 1-dimensional compression (oedometer) test is probably still the most common type of test for the provision of settlement calculation data. As an illustration, Fig. 5 shows the NTH-type consolidometer constructed for continuous loading tests.

Consolidation tests provide log (stress)-strain or stress-strain plots. The linear plot enables a convenient evaluation of the tangent modulus (constrained modulus). Janbu (1963) suggested that the tangent modulus (M) of most soils may be represented by the formula

$$M = m p_a \left(\frac{\sigma'}{p_a}\right)^{1-a} \quad \ldots\ldots\ldots\ldots\ldots\ldots\ldots\ldots\ldots\ldots \quad (1)$$

where m = modulus number
p_a = reference stress, usually 10 kPa
σ' = axial effective stress
a = constant in the range 0 to 1

The parameters m and a[1] are constants for a given soil.

One of the moduli included in the more general soil model presented herein, is related to the constrained modulus defined above.

More thorough information of the behaviour of a soil sample is gained from a triaxial test. Figure 6 demonstrates one of the more sophisticated triaxial apparatuses developed for axi-symmetrical testing.

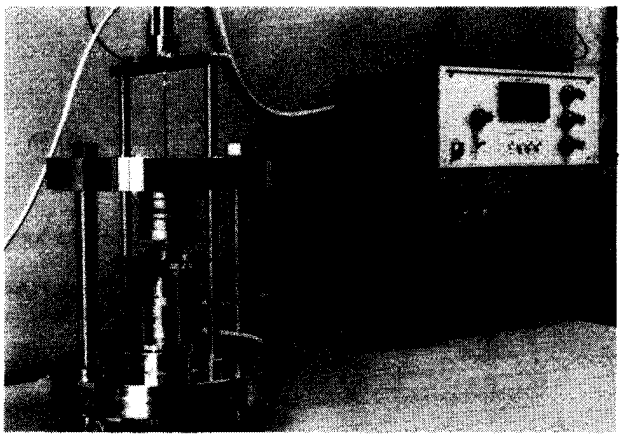

Fig. 5. Consolidometer for continuous loading consolidation tests, developed at the Norwegian Institute of Technology (NTH).

[1] Not to be confused with the attraction defined in Eq. 2.

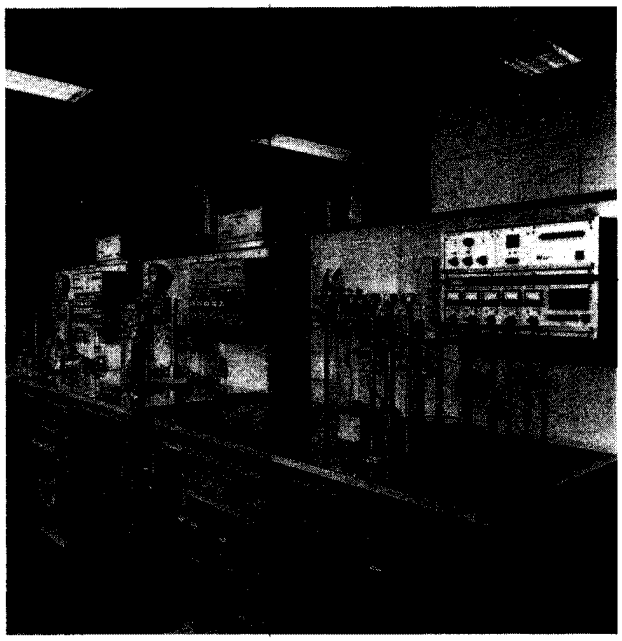

Fig. 6. Automatic triaxial testing equipment developed in partnership by Geonor A/S and the Norwegian Institute of Technology (NTH).

Originally, the triaxial apparatus was basically used for the determination of strength parameters. As stress-strain models developed, triaxial devices gradually became more useful as they provided information about stresses and strains. Stress paths from these tests supply an overview of testing conditions, results and behaviour of a soil sample.

In Fig. 7, the effective stress paths of triaxial compression tests on clay and sand are drawn; in all tests shearing of the samples is done under constant volume or nearly constant volume conditions (undrained).

The mobilized Mohr-Coulomb friction angle has proved to be a most instructive parameter or stress function; the following definition applies:

$$\sin\rho = \frac{\frac{1}{2}(\sigma_1' - \sigma_3')}{\frac{1}{2}(\sigma_1' + \sigma_3') + a} \quad \ldots\ldots\ldots\ldots\ldots\ldots\ldots\ldots\ldots\ldots \quad (2)$$

where $a = c/\tan\varphi$ is the attraction[2]. If σ_1' and σ_3' are failure stresses, then $\rho = \varphi$ and the full Mohr-Coulomb friction angle is mobilized, cfr. Fig. 2.

Figure 8 redraws the stress paths in Fig. 7 in terms of mobilized Mohr-Coulomb friction versus axial strain. The attraction, a, has been carefully selected so as to best fit the test results over the stress range in question, cfr. Fig. 7. Figure 8 demonstrates for each soil a fairly unique relation between mobilized friction and axial strain. Figure 7 also illustrates this as straight concentric lines represent approximately equal axial strain; the magnitude of axial strain is given at points along the stress paths.

[2] Note that for simplicity no mark (') appears together with a, c, φ, ρ etc. to indicate effective stress parameters as such are exclusively dealt with.

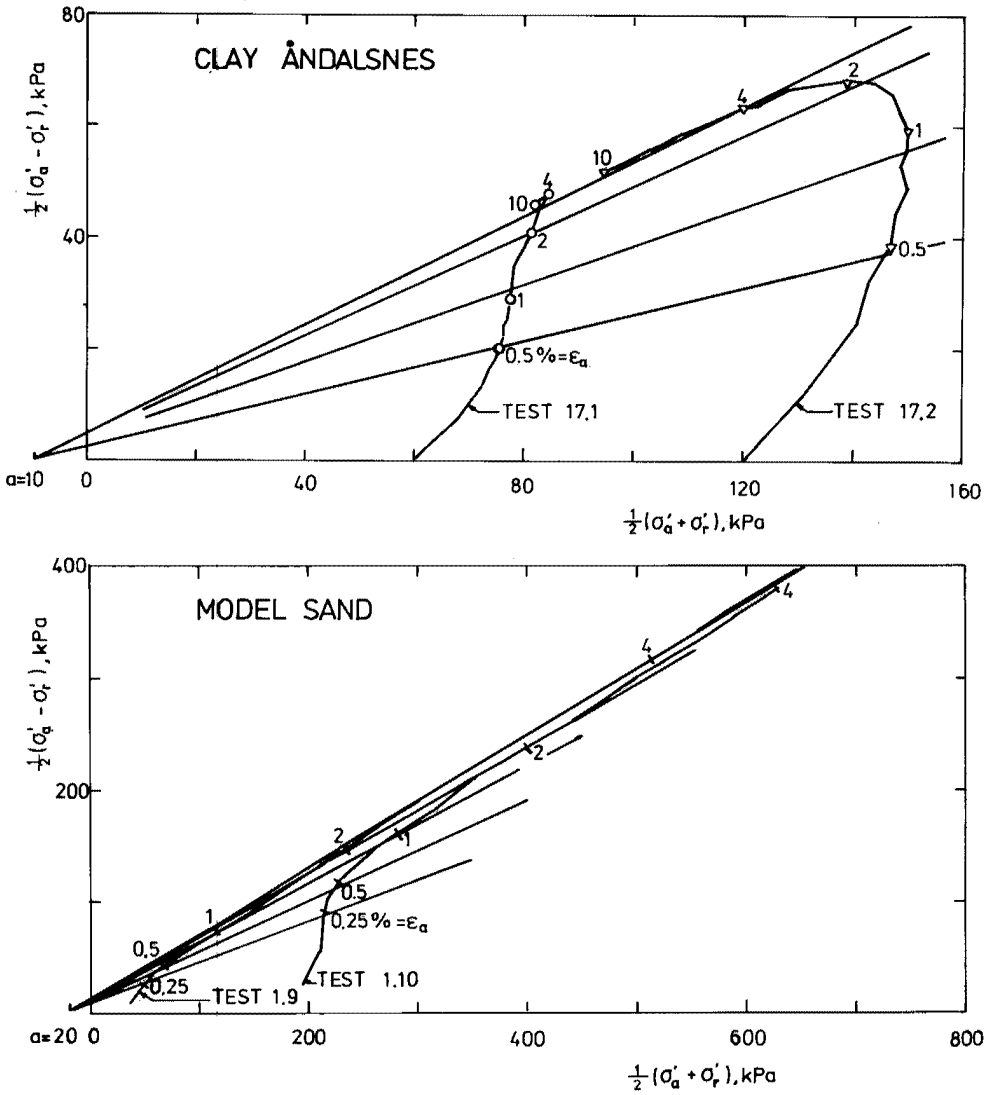

Fig. 7. Triaxial compression tests on clay (undrained) and sand (constant volume).

Similar approximate uniqueness has previously been documented by Lambe (1964) for three normally consolidated clays. Janbu (1973) extended the concept to include sand. He also introduced the degree for shear mobilization

$$1/F = \tan\rho/\tan\varphi \quad \ldots\ldots (3)$$

where F is a safety factor. Hence a relation between safety factor and strain level is pointed out.

Also the tests on Model Sand made by the lecturer (32) support the concept of uniqueness between mobilized friction and axial strain.

The behaviour of heavily overconsolidated (OC) clays is more questionable. For such clays the overconsolidation ratio (OCR) and the maximum past pressure (p_c') are believed to influence strongly on the attraction (a) or the cohesion intercept (c). As a result, the attraction likely becomes increasingly stress-dependent as the OCR increases. It is however believed that with an appropriate choise of attraction, the concept may work when considering a limited stress range.

Uniqueness between mobilized friction and axial strain, or more correctly deviatoric strain, under undrained shear is another cornerstone of the model presented herein.

CONCEPTUAL IDEA

In the analysis of soil deformation behaviour, it is convenient to separate deformation into volume change and distortion as illustrated in Fig. 9.

The volumetric and deviatoric strains are defined in terms of the principal strains by

$$\epsilon_v = \epsilon_1 + \epsilon_2 + \epsilon_3 \quad \ldots\ldots (4)$$

$$\epsilon_d = \epsilon_1 - \epsilon_3 \quad \ldots\ldots (5)$$

When disregarding inherent anisotropy, one can represent all the possible states of deformation of triaxial (axisymmetrical) samples by a combination of the two strain components or strain functions named above.

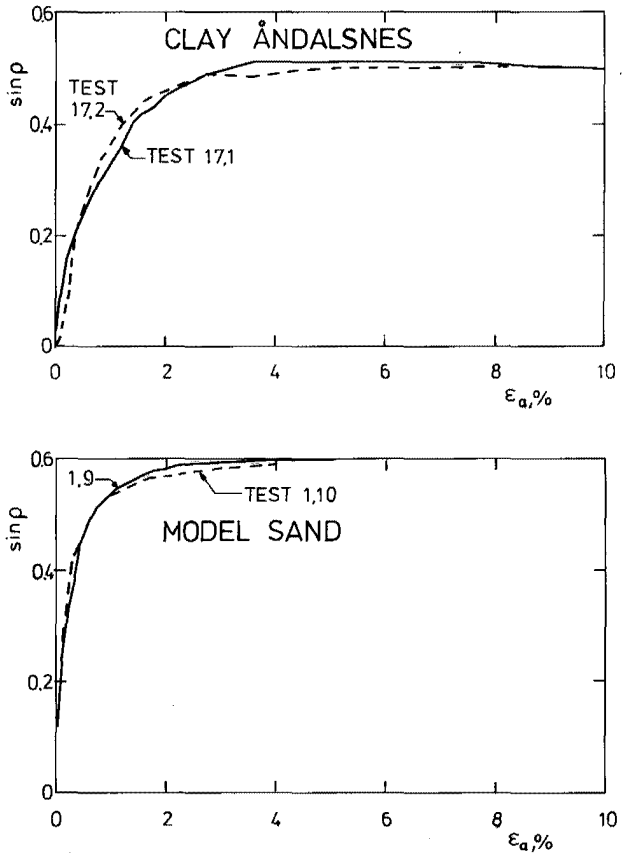

Fig. 8. Mobilized Mohr-Coulomb friction (sinρ) versus axial strain (ϵ_a) in triaxial compression, redrawn from Fig. 7.

The behaviour of an isotropic, linear-elastic material may be described in terms of the following two relations:

$$\tau = G\gamma \quad \ldots\ldots (6)$$

$$\sigma_m = K\epsilon_v \quad \ldots\ldots (7)$$

where G is the shear modulus and K is the bulk modulus. The former equation states a unique relation between shear stress (τ) and shear strain (γ) regardless of the coordinate system, including also

$$\tfrac{1}{2}(\sigma_1 - \sigma_3) = G\epsilon_d \quad \ldots\ldots (8)$$

which relates the maximum shear stress to the maximum shear strain.

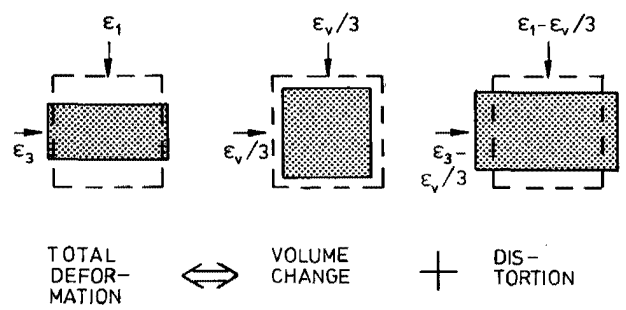

Fig. 9. Components of deformation.

Equation 7 establishes a unique relation between mean normal stress (σ_m) and volumetric strain (ϵ_v).

Figure 10a demonstrates the properties of the isotropic, linear-elastic material. Straight vertical and horizontal lines refer to equal volumetric and deviatoric strains respectively. The elastic material named "solids" in the figure may furthermore obey the Tresca failure criterion which appears as a straight horizontal line in the figure.

Now, let us see how soil behaviour fits into this picture. First we recognize the Mohr-Coulomb failure line as being inclined in Fig. 10b. We also notice that σ_m has been traded with $\frac{1}{2}(\sigma_1' + \sigma_3')$ in the lower figure in order to suit with the Mohr-Coulomb failure criterion.

It has been pointed out earlier that significant experimental evidence indicated straight concentric lines of equal axial strain under undrained triaxial compression. This also implies the existence of straight lines of equal deviatoric strain (ϵ_d) as illustrated in the figure.

The crucial question is whether unique lines of equal deviatoric strain represent a general feature of soil behaviour, also under loading conditions others than undrained triaxial compression.

First it is easy to convince oneself that straight lines of equal *deviatoric* strain are more likely than lines of equal *axial strain* as a general feature. One argument is the apparent similarity to the elastic material. More con-

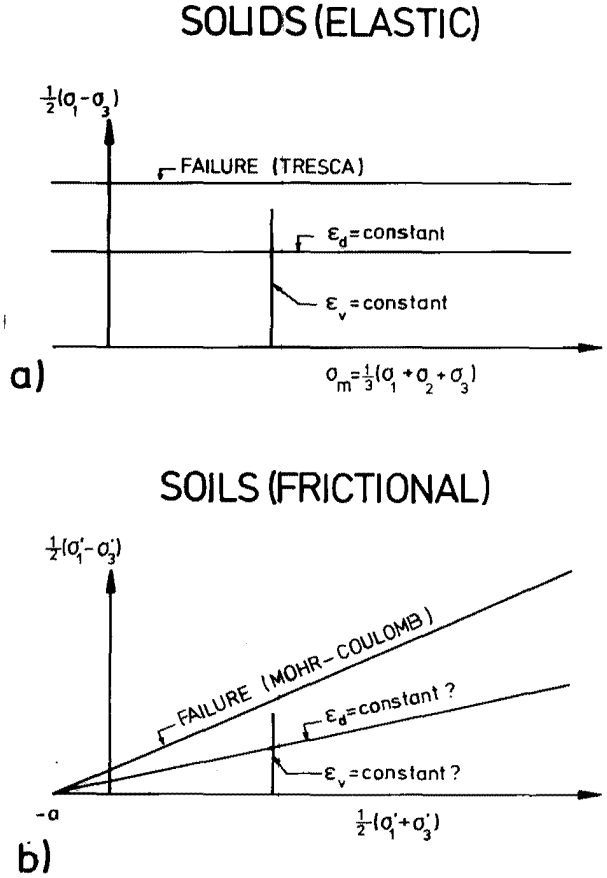

Fig. 10. Patterns of deformation of solids and soils.

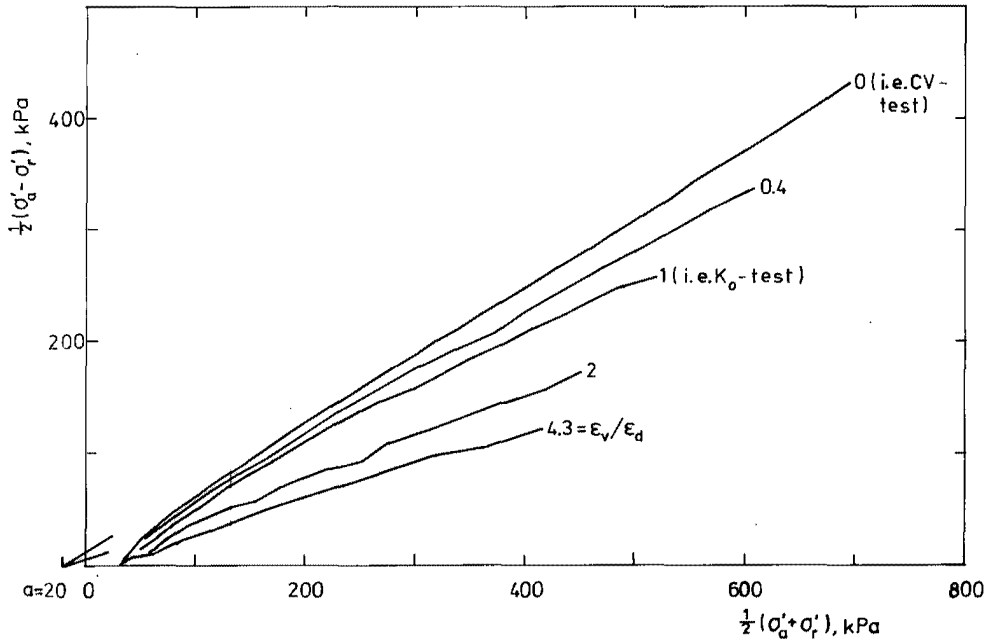

Fig. 11. Effective stress paths of triaxial compression tests on Model Sand under various ratios ϵ_v/ϵ_d.

vincing is, however, the case of hydrostatic compression, i.e. a stress path along the horizontal axis. If one assumes isotropic behaviour, volumetric strain only will take place. Hence the horizontal axis is a line of equal (zero) deviatoric strain. Axial straining is, however, taking place during hydrostatic compression. Therefore the hydrostatic axis cannot possibly be a line of equal axial strain.

Unfortunately it is also easy to convince oneself that straight concentric lines may not always correspond to equal deviatoric strain. For instance in the K_o-consolidation test, i.e. no lateral strain may take place, the stress path after some shearing likely becomes a straight line of constant mobilized friction.

The deviatoric strain is of course not constant during one-dimensional compression as $\epsilon_v/\epsilon_d = 1$.

More general, Fig. 11 shows effective stress paths of triaxial compression tests run under various ratios ϵ_v/ϵ_d between volumetric and deviatoric strain. To each ratio ϵ_v/ϵ_d the stress path seems to approach a straight line of constant mobilized friction. The K_o-consolidation test ($\epsilon_v/\epsilon_d = 1$), the constant volume (CV) compression test ($\epsilon_v/\epsilon_d = 0$) and the hydrostatic compression test ($\epsilon_v/\epsilon_d = \infty$) are in fact all well known special cases under which stress paths tend to approach lines of equal mobilized friction.

For soils, there is nor a straight forward relation between mean stress and volumetric strain as for truly elastic materials. One complicating factor is the absence of the intermediate principal stress σ_2' in the Mohr-Coulomb failure criterion. Another is the tendency of soil to dilate or contract during shearing. Hence lines of equal volumetric strain corresponding to constant effective mean stress may not be expected for soils.

In a general soil model, consideration must also be given to stress history, inherent anisotropy, stress induced anisotropy, rotation of the principal stress directions and the magnitude of the intermediate principal stress. Still it may be useful as a conceptual idea to think of soil behaviour in terms of Fig. 10b; on one hand, linking mobilized Mohr-Coulomb friction together with deviatoric strain, and on the other hand linking mean stress with volumetric strain. As pointed out above, this concept is too simple for a general soil model. Some modifications are necessary in order to obtain a more realistic soil model.

SOIL MODEL UNDER AXISYMMETRICAL STRESSES

Based on the simple soil deformation concept above, a more general soil stress-strain-strength model shall now be constructed. Instead of presenting the full model at once, we shall start with the simplified model applying to triaxial (axisymmetrical) compression under fixed principal stress directions. Thereafter the model shall be extended stepwise to include all independent principal stresses and arbitrary principal stress directions. The theory and test results presented refer to the work reported in Ref. 32.

The axisymmetrical case model is written

$$d\sigma_m' = M_k d\epsilon_v + M_d d\epsilon_d \quad \ldots\ldots\ldots\ldots\ldots\ldots\ldots\ldots \quad (9)$$

$$df_s = -f_s M_o d\epsilon_v + M_g d\epsilon_d \quad \ldots\ldots\ldots\ldots\ldots\ldots\ldots\ldots \quad (10)$$

Four resistance moduli are involved;

M_k = compression modulus
M_d = dilatancy modulus
M_g = distortion modulus
M_o (no name suggested).

The former two moduli have the unit of stress, while the latter two are non-dimensional.

The variables $d\sigma_m'$, $d\epsilon_v$ and $d\epsilon_d$ are respectively increments of mean effective stress, volumetric strain and deviatoric strain.

Finally, f_s is the degree of mobilized friction (Mohr-Coulomb) defined by

$$f_s = \sin\rho / \sin\varphi \quad \ldots\ldots (11)$$

or combined with Eq. 2:

$$f_s = \frac{1}{\sin\varphi} \frac{\frac{1}{2}(\sigma_1' - \sigma_3')}{\frac{1}{2}(\sigma_1' + \sigma_3') + a} \quad \ldots\ldots (12)$$

The definition above differs slightly from the one given by Janbu (1973) and quoted in Eq. 3. Equations 11 and 12 normalize the mobilized Mohr-Coulomb friction ($\sin\rho$) in the range 0 to 1.

We shall first investigate whether the model complies with the deformation concept in the preceding section and then determine values of the moduli from available test results. Only a few aspects of the model will be focused on, as an examination of all its capabilities would prove too lengthy. For further examination of the model and exhaustive test results Ref. 32 is referred to.

Test results and behaviour under loading conditions (virgin loading) are primarily examined herein, whereas Ref. 32 also provides test results and further details regarding unloading conditions.

At first thought it is natural to define loading conditions in terms of increasing values of f_s and σ_m'. However, there are some good reasons for relating the definition of loading to the values of the strain increments $d\epsilon_d$ and $d\epsilon_v$. As illustrated in Fig. 12, these values are either positive or negative depending on the direction of the effective stress path at a given state of stress. According to the selected definition, the moduli M_d and M_g take loading values for $d\epsilon_d \geq 0$, whereas loading values of M_v and M_o apply for $d\epsilon_v \geq 0$.

When comparing Eqs. 6, 7, 9 and 10, we at once recognize the apparent similarity between the compression modulus (M_k) and the bulk modulus (K), and between the distortion modulus (M_g) and the shear modulus (G).

However, the maximum shear stress $\frac{1}{2}(\sigma_1 - \sigma_3)$ expressed in elasticity theory is traded with the degree of mobilized friction f_s. This allows for concentric lines of equal deviatoric strain in undrained shearing. The introduction of f_s also makes it easy to encounter the Mohr-Coulomb failure criterion.

The Model Sand

The tests referred to are all made on Model Sand, a medium to coarse sand. The building-in porosity of the

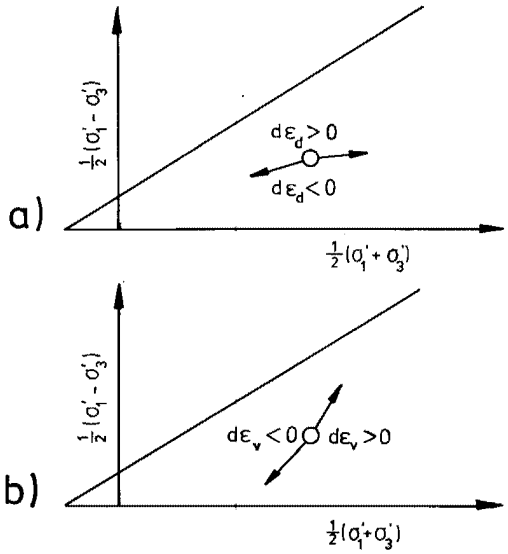

Fig. 12. Definition of loading related to the direction of the strain increments.
a) M_d and M_g: loading when $d\epsilon_d \geq 0$
b) M_o and M_k: loading when $d\epsilon_v \geq 0$

samples was approximately 40%, indicating a dense consistency. As an overall result of isotropically consolidated drained tests (CID) and isotropically consolidated constant volume tests (CICV), all under triaxial compression, the Mohr-Coulomb strength parameters were estimated as follows:

a = 20 kPa (attraction)
$\sin\varphi$ = 0.61 (φ = 38°)

It may seem surprising to some that non-zero attraction or cohesion is specified for sand. However, the attraction is not considered a physical constant for the sand, valid under all possible stresses, including very small or even negative stresses. Rather the attraction is considered a convenient parameter chosen so as to best fit the test results over the stress range in consideration.

Resistance to Shearing

Under constant volume ($d\epsilon_v = 0$), Eq. 10 reduces to

$$df_s = M_g d\epsilon_d \quad \ldots\ldots (13)$$

implying

$$M_g \sin\varphi = d\sin\rho / d\epsilon_d \quad \ldots\ldots (14)$$

The latter equation is suitable for the determination of M_g from test results. Figure 13 summarizes the results of isotropically consolidated, constant volume triaxial compression tests (CICV).

In Fig. 13, the test results are divided into two groups depending on the magnitude of the consolidation stress σ_c'. The consolidation stress appears to have no significant influence on M_g. This is consistent with a unique relation between mobilized friction and deviatoric strain, implying also straight concentric lines of equal deviatoric strain as illustrated in Fig. 10b.

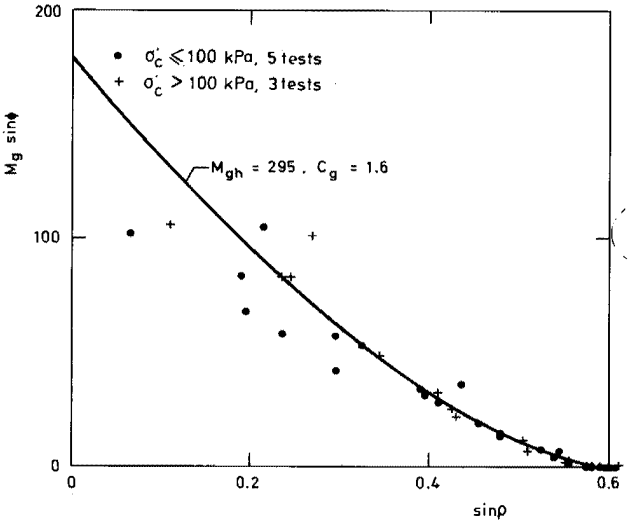

Fig. 13. Distortion modulus M_g times $\sin\varphi$ versus mobilized friction ($\sin\rho$) from CICV-tests on Model Sand.

The following formula was chosen to fit the test results:

$$M_g = M_{gh}(1-f_s)^{C_g} \quad \ldots\ldots (15)$$

where M_{gh} = 295 (value of M_g under hydrostatic stress)
C_g = 1.6 (exponent)

Under unloading, the limited number of tests done so far have indicated $M_g = M_{gh}$ regardless of stress state. This is a not very surprising finding, indicating some kind of elastic or quasi-elastic behaviour during loading conditions at near-hydrostatic stresses and during unloading.

Resistance to Compression

The compression modulus M_k is most conveniently determined from hydrostatic compression tests. For a soil deforming isotropically ($d\epsilon_d = 0$), Eq. 9 reduces to

$$d\sigma_m' = M_k d\epsilon_v \quad \ldots\ldots (16)$$

or

$$M_k = d\sigma_m'/d\epsilon_v \quad \ldots\ldots (17)$$

Once the dilatancy modulus M_d is determined, M_k may also be estimated from the relation

$$M_k = \frac{d\sigma_m'}{d\epsilon_v} - \frac{M_d}{d\epsilon_v/d\epsilon_d} \quad \ldots\ldots (18)$$

which is a reformulation of Eq. 9.

Unless the ratio $d\epsilon_v/d\epsilon_d$ is small ($\ll 1$), the last term of Eq. 18 is likely to be much smaller than the first one. When comparing M_k with the elastic bulk modulus K, one might perhaps say that M_k is a quasi-elastic bulk modulus corrected for dilatancy.

In Fig. 14, both of the above relations were used to calculate M_k; the latter equation applied to strain controlled tests run under various ratios of $d\epsilon_v/d\epsilon_d$. The rather moderate scatter in the results is comforting, especially since stress paths close to failure are also included among the tests. In such tests, small values of $d\epsilon_v/d\epsilon_d$ appeared, implying significant dilatancy. The results justify the determination of M_k from hydrostatic compression tests alone.

The test results presented are fitted by the formula

$$M_k = m_k p_a \left[\frac{\sigma_m' + a}{p_a}\right]^{C_k} \quad \ldots\ldots (19)$$

where m_k = 180 (compression modulus number)
C_k = 0.7 (exponent)
a = 20 kPa (attraction)
p_a = 100 kPa (reference stress)

The above formula for M_k is similar to the formula for the constrained modulus suggested by Janbu, cfr. Eq. 1.

The form of Eq. 19 applies to unloading as well. The plot of M_k-values of unloading tests fitted very well to a straight line ($M_k = 220$, $C_k = 1$).

Note that M_k depends on σ_m' only, whereas M_g appears to be a function of f_s only. This feature is in fact the key point in describing soil behaviour in terms of stress and strain functions such as f_s, σ_m', ϵ_d and ϵ_v.

The parameters M_g and M_k are the two most important of the suggested soil model. The observed dependency of these moduli on f_s and σ_m' supports the simple soil deformation concept illustrated in Fig. 10b.

The remaining two parameters M_o and M_d are necessary in order to overcome some of the oversimplifications of the simple deformation concept just referred to. The dilatancy modulus M_d naturally accounts for dilatancy while the parameter M_o allows for deviatoric strains taking place for instance under K_o-consolidation.

Dilatancy

The isotropic, linear elasticity theory suggests that the mean stress σ_m' is independent of the deviatoric strain ϵ_d

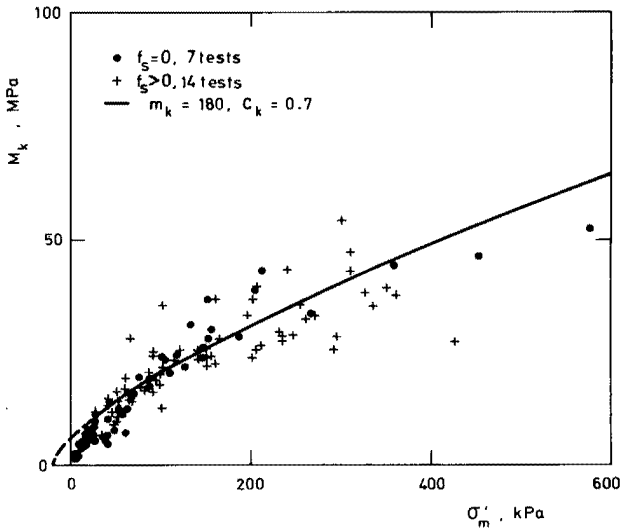

Fig. 14. Compression modulus (M_k) versus mean stress (σ_m') from strain-ratio controlled triaxial compression tests on Model Sand.

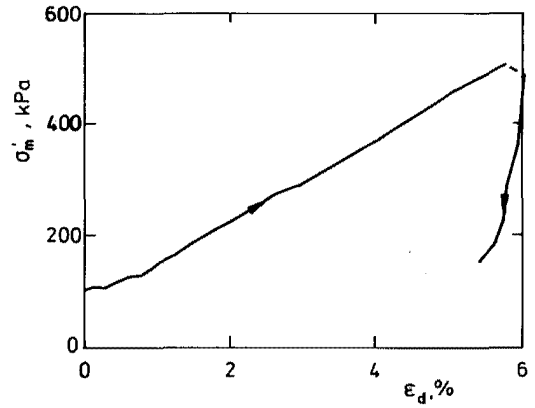

Fig. 15. Mean stress versus deviatoric strain of a CICV-test on Model Sand under loading and unloading.

for loading under constant volume ($d\epsilon_v = 0$). Due to dilatancy this is as a general rule not true for soils. Certainly it is not true for the Model Sand as Fig. 15 demonstrates.

The dilatancy modulus M_d is most conveniently determined from constant volume tests for which Eq. 9 reduces to

$$d\sigma_m' = M_d d\epsilon_d \quad \ldots\ldots (20)$$

or

$$M_d = d\sigma_m'/d\epsilon_d \quad \ldots\ldots (21)$$

Figure 16 shows the results of a number of constant volume triaxial compression (CICV) tests. Different symbols refer to high and low values of the consolidation stress σ_c'. The results seem fairly insensitive to mean stress. The scatter of the test results under moderate and low mobilized friction must be considered in view of the difficult testing conditions, i.e. keeping the volume precisely constant during the shearing of a dense sand.

One may question the appropriateness of fitting the results by a straight line as indicated. However, it should be emphasized that the magnitude of M_d is not very important until the mobilized friction becomes high and significant shear strain takes place.

It is suggested to put $M_d = 0$ for hydrostatic stresses, which is a requirement for isotropic behaviour under hydrostatic stresses. Without going into detail at this point, this is suggested for several reasons.

The modulus M_d has also been determined from drained triaxial compression tests (CID) in which the radial stress (σ_3') has been kept constant during shearing. At near-failure stresses, the samples yielded under nearly constant stress, i.e. $d\sigma_m' \simeq 0$, for which Eq. 9 may be rewritten as follows:

$$M_d \simeq M_k d\epsilon_v/d\epsilon_d \quad \ldots\ldots (22)$$

The results of five CID-tests thus interpreted are shown in Fig. 17.

Clearly, the results reveal M_d depending on mean stress. Thus M_d does not seem to be unique under all modes of loading.

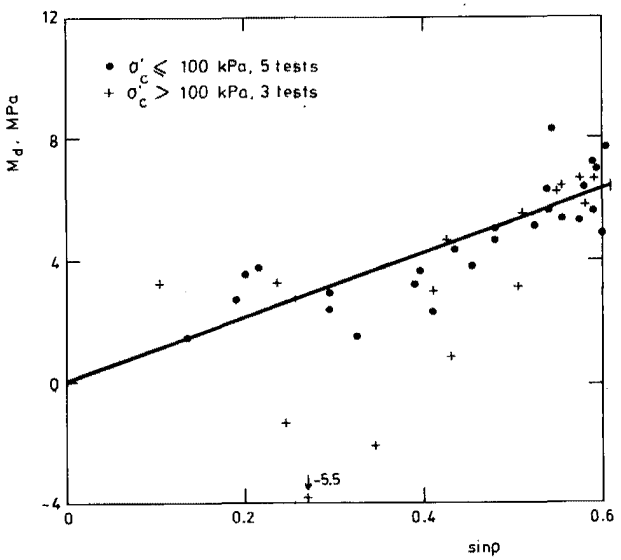

Fig. 16. Dilatancy modulus (M_d) versus mobilized friction (sinρ) from CICV-tests on Model Sand.

Based on all tests, M_d appears to depend on both f_s and σ_m'. The following formula is suggested for the Model Sand:

$$M_d = m_d p_a f_s^{C_{df}} \left[\frac{\sigma_m' + a}{p_a}\right]^{C_d} \quad \ldots\ldots (23)$$

with the following parameter values:

m_d = 36 (dilatancy modulus number)
C_{df} = 1 (exponent)
C_d = 0.7 (exponent)
a = 20 kPa (attraction)
p_a = 100 kPa (reference stress)

Except the f_s-term, the formulas for M_k and M_d are similar.

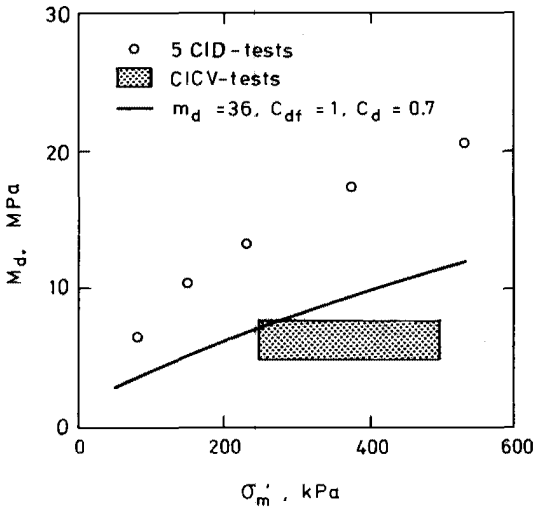

Fig. 17. Dilatancy modulus (M_d) at near-failure stresses from CID- and CICV-tests on Model Sand.

Noteworthy, the values of the exponents C_d and C_k are found equal, resulting in a ratio M_d/M_k not depending on the mean stress σ_m'.

The scatter of the test results and the apparent lack of uniqueness of M_d may seem uncomfortable. However, it should be kept in mind that many soil models in use today simply disregard dilatancy. In that respect even a rough estimate of M_d is a step forwards.

Noteworthy also is that M_d was non-zero during unloading; the value of M_d was even larger than during loading. The tests on Model Sand indicated a linear relation between M_d and σ_m' with the following parameters referring to Eq. 23: $m_d = 200$, $C_{df} = 0$ and $C_d = 1$.

The Parameter M_o

As pointed out earlier, the fourth parameter M_o is needed for instance to allow for deviatoric strain taking place during compression under constant mobilized friction. The appropriate interpretation formula is derived from Eq. 10:

$$M_o \sin\rho = \frac{M_g \sin\varphi - d\sin\rho/d\epsilon_d}{d\epsilon_v/d\epsilon_d} \quad \ldots\ldots\ldots\ldots\ldots\ldots \quad (24)$$

The interpretation is greatly simplified for constant mobilized friction conditions. Then $d\sin\rho = 0$ leads to

$$M_o \sin\rho = \frac{M_g \sin\varphi}{d\epsilon_v/d\epsilon_d} \quad \ldots\ldots\ldots\ldots\ldots\ldots\ldots\ldots \quad (25)$$

Figure 11 showed the stress paths of a number of strain controlled triaxial compression tests. In each test the ratio $d\epsilon_v/d\epsilon_d$ was kept constant. The K_o-consolidation, under which $d\epsilon_v/d\epsilon_d = 1$, is one such test. As expected from the experience with K_o-tests, all stress paths in Fig. 11 tend to approach straight lines of constant mobilized friction. The actually mobilized friction in each test is a result of the strain increment ratio $d\epsilon_v/d\epsilon_d$ applied.

Figure 18 shows test results of Model Sand. A constant $M_o = 38$ is the best estimate based on all results available. Considerable scatter of the results is caused by problems in keeping the ratio $d\epsilon_v/d\epsilon_d$ constant during testing, mostly owing to false deformations in the triaxial apparatus. This problem is overcome in some of the tests in which the false deformations were accounted for during compression. Thus results marked with black dots in the figure should be given most consideration. The improved testing procedure appears to reduce the scatter of the results.

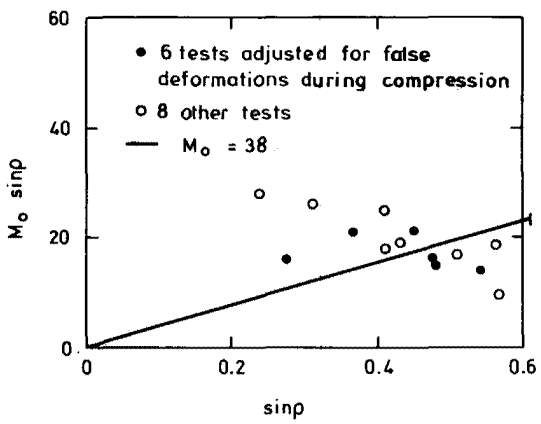

Fig. 18. Parameter M_o times mobilized friction ($\sin\rho$) versus mobilized friction from triaxial compression tests on Model Sand, run under various strain increment ratios.

The lecturer assumes that a constant value of M_o is accurate enough for most applications of the model. Thus it should not be necessary to run tests under various ratios $d\epsilon_v/d\epsilon_d$ in order to determine M_o; K_o-tests will suffice.

Finally, some unloading tests have been performed under constant mobilized friction. Practically no shear deformation took place under unloading, indicating $M_o = 0$ according to the interpretation formula (Eq. 25).

Prediction of Results from Triaxial Tests

Since triaxial tests have been interpreted to estimate all moduli and parameters of the model, the use of the model to predict the behaviour in the same tests may hardly be considered true predictions. Nevertheless, it may be interesting to use the model to backcalculate one or two stress paths to see exactly what they look like.

Figure 19 presents the test results and predictions of K_o- and CICV-tests. As expected, the agreement is reasonable.

MODEL EXTENDED TO THREE DIMENSIONS

The model presented so far has been restricted to axisymmetrical stresses where two of the principal stresses are equal. The inclusion of the intermediate principal stress σ_2' calls for a third stress function in addition to the mean stress σ_m' and the degree of mobilized friction f_s. The third stress function defines the relative magnitude of the intermediate principal stress;

$$b = \frac{\sigma_2' - \sigma_3'}{\sigma_1' - \sigma_3'} \quad \ldots\ldots\ldots\ldots\ldots\ldots\ldots\ldots\ldots\ldots \quad (26)$$

Correspondingly, the state of strain must be described in terms of all three principal strains or three functions thereof. The volumetric and deviatoric strains ϵ_v and ϵ_d ($= \epsilon_{d13}$) are already defined. In addition comes another deviatoric strain component defined by

$$\epsilon_{d23} = \epsilon_2 - \epsilon_3 \quad \ldots\ldots\ldots\ldots\ldots\ldots\ldots\ldots\ldots\ldots \quad (27)$$

Figure 20 defines mobilized friction and deviatoric strains in Mohr diagrams.

In the previous section, the degree of mobilized friction f_s on the plane of most mobilized friction was linked together with the largest deviatoric strain ϵ_d. When linking together one of the minor deviatoric

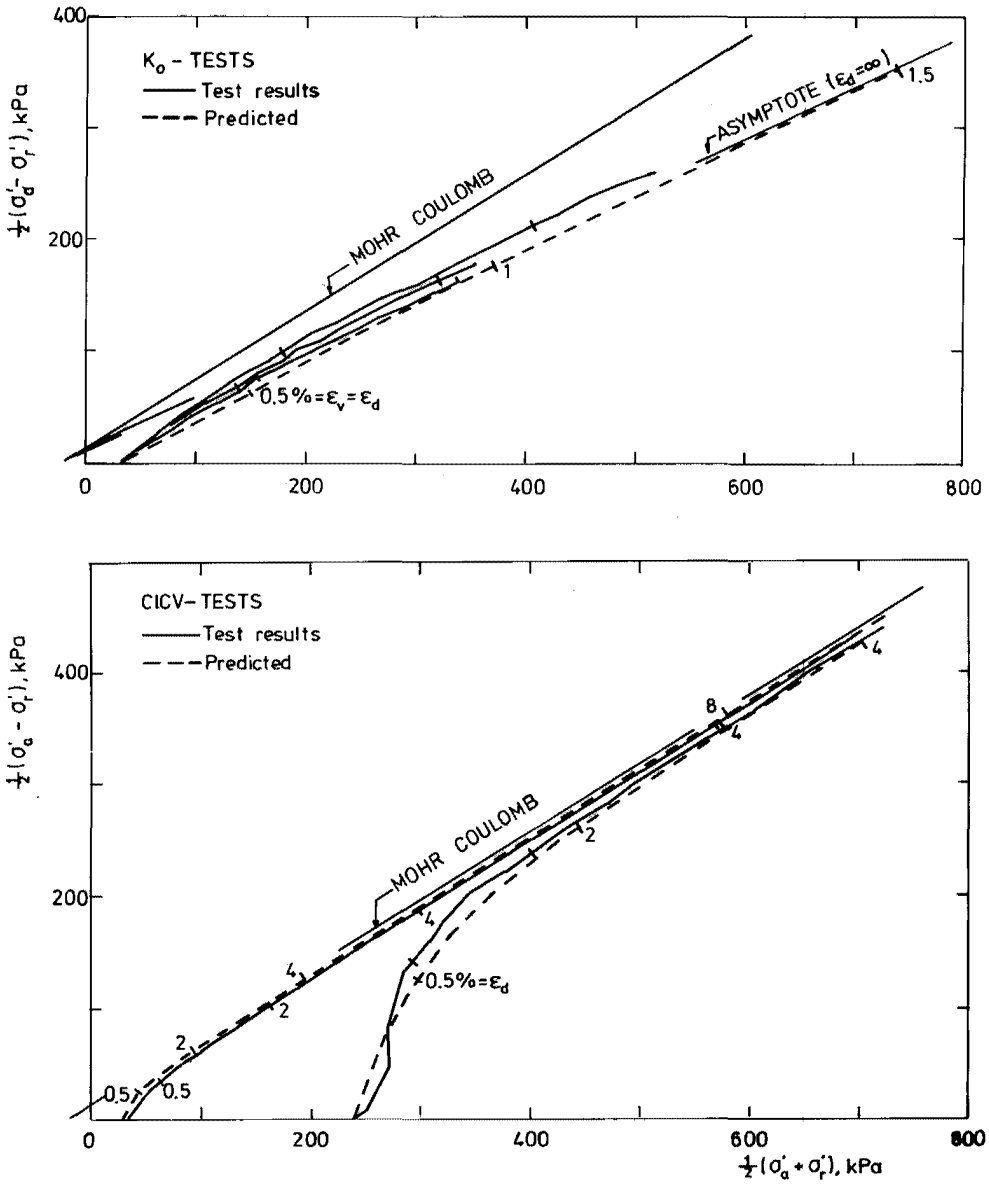

Fig. 19. Test results and predicted (back-calculated) effective stress paths of K_o-consolidation tests and CICV-tests.

strains ϵ_{d23} and the corresponding degree of mobilized friction $f_{s23} = bf_s$, one gets

$$d(bf_s) = -bf_s M_o d\epsilon_v + M_g d\epsilon_{d23} \quad \ldots\ldots\ldots\ldots\ldots\ldots \quad (28)$$

Recalling also Eqs. 9 and 10, one can write the constitutive relation for independent principal stresses and restricted to fixed principal stress directions as:

$$d[\sigma_m' \; f_s \; bf_s]^T = \mathbf{M}\, d[\epsilon_v \; \epsilon_{d13} \; \epsilon_{d23}]^T \quad \ldots\ldots\ldots\ldots\ldots\ldots \quad (29)$$

in which the matrix

$$\mathbf{M} = \begin{bmatrix} M_k & M_d & 0 \\ -f_s M_o & M_g & 0 \\ -bf_s M_o & 0 & M_g \end{bmatrix} \quad \ldots\ldots\ldots\ldots\ldots\ldots \quad (30)$$

Equation 29 is a relation between the increments of the principal stress and strain functions. It may be transformed into the following relation between the increments of the principal stresses and strains:

$$d[\sigma_1' \; \sigma_2' \; \sigma_3']^T = \mathbf{T}_\sigma^{-1} \mathbf{M} \mathbf{T}_\epsilon d[\epsilon_1 \; \epsilon_2 \; \epsilon_3]^T \quad \ldots\ldots\ldots\ldots\ldots\ldots \quad (31)$$

where the transformation matrices $\mathbf{T}_\sigma^{-1}$ and $\mathbf{T}_\epsilon$ are given in Appendix.

Now let us look a bit further into the model. No additional modulus or soil parameter has been added when extending the model to include three independent principal stresses. Thus triaxial compression tests are in the principle still sufficient for the determination of all parameters.

As the model has not been tested under stress conditions for which σ_2' differs from σ_3', further testing will have to decide to what extent the parameters are unique.

The model uses the Mohr-Coulomb friction angle as a parameter. At least the moderate lack of uniqueness of

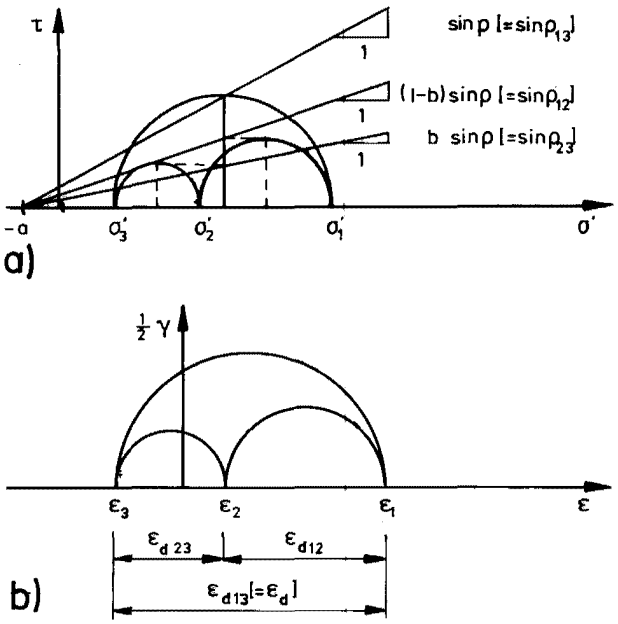

Fig. 20. Definitions of a) mobilized friction and b) deviatoric strains.

the friction angle must have influence on the uniqueness of the model.

One comforting aspect is, however, the way in which the intermediate principal stress and strain appear in the model. The Equations 10 and 28 are both derived from the following more general equation relating an increment of the degree of mobilized friction to increments of volumetric and deviatoric strains:

$$df_{sij} = -f_{sij}M_o d\epsilon_v + M_g d\epsilon_{dij} \quad \ldots\ldots (32)$$

where

$$f_{sij} = \frac{\sin\rho_{ij}}{\sin\varphi} = \frac{1}{\sin\varphi}\,\frac{\frac{1}{2}(\sigma_i' - \sigma_j')}{\frac{1}{2}(\sigma_1' + \sigma_3') + a} \quad \ldots\ldots (33)$$

$$\epsilon_{dij} = \epsilon_i - \epsilon_j \quad \ldots\ldots (34)$$

and i, j = 1, 2 or 2, 3 or 1, 3

as illustrated in Fig. 20. Substituting of f_{s13} with f_s for simplicity, and since $f_{s23} = bf_s$, Eqs. 10 and 28 are seen to be both deduced from Eq. 32. One basic principle thus relates increments of mobilized friction and deviatoric strain. No additional concept is needed to include the intermediate principal stress and strain increments.

In Eq. 9, only the largest deviatoric strain component ϵ_d (= ϵ_{d13}) is involved. It may therefore seem like not all components of deviatoric strain affect dilatancy in the same manner. This is, however, not true as Eq. 9 may be rewritten into:

$$d\sigma_m' = M_k d\epsilon_v + \tfrac{1}{2}M_d(d\epsilon_{d12} + d\epsilon_{d23} + d\epsilon_{d13}) \quad \ldots\ldots (35)$$

recalling that $\epsilon_{d13} = \epsilon_{d12} + \epsilon_{d23}$ (cfr. Fig. 20b).

In view of Eq. 31, one might ask why not define a relation between increments of principal stresses and strains in the first place. However, each modulus or coefficient in the composite matrix $\mathbf{T}_\sigma^{-1}\mathbf{M}\mathbf{T}_\epsilon$ is an extremely involved function of the state of stress. Equation 29, on the other hand, relates increments of functions of stresses and strains reflecting basic aspects of soil behaviour. Therefore the parameters involved may readily be estimated from conventional triaxial tests.

GENERAL MODEL

So far fixed principal stress directions have been assumed, implying also principal directions of strain coinciding with those of stress. In the general case, the principal directions of stress rotate and the principal directions of stress and strain no longer coincide. Nor need the principal directions of the stress and strain increments coincide. Altogether there are four sets of principal directions involved, and none of them need coincide.

Although the present model does not separate deformation explicitly into elastic and plastic components, the model is basically resting on plasticity concepts. The lines of equal mobilized friction in the Mohr diagram are comparable with yield surfaces in plasticity theory. From the test results presented as well as through the experience summarized above, we know that the distortion modulus M_g will likely decrease to zero as the mobilized friction increases until failure. However, once loading is reversed, M_g suddenly increases to roughly M_{gh}, which is the value of M_g at hydrostatic stress.

As in plasticity theory, stress changes should be separated into loading, neutral stress changes and rebound.

The general model separates an incremental stress change into incremental changes of the principal stresses and rotation of the principal stress directions. In order to do so a local coordinate system is defined with axes α, β and γ coinciding with the instantaneous directions of σ_1', σ_2' and σ_3'.

The stress functions are then written

$$\sigma_m' = \tfrac{1}{3}(\sigma_\alpha' + \sigma_\beta' + \sigma_\gamma') \text{ (= stress invariant)} \quad \ldots\ldots (36)$$

$$f_s = \frac{1}{\sin\varphi}\,\frac{\frac{1}{2}(\sigma_\alpha' - \sigma_\gamma')}{\frac{1}{2}(\sigma_\alpha' + \sigma_\gamma') + a} \quad \ldots\ldots (37)$$

$$b = \frac{\sigma_\beta' - \sigma_\gamma'}{\sigma_\alpha' - \sigma_\gamma'} \quad \ldots\ldots (38)$$

where φ still is the Mohr-Coulomb friction angle and $a = c/\tan\varphi$ is the attraction.

Furthermore, the strain functions are written

$$\epsilon_v = \epsilon_\alpha + \epsilon_\beta + \epsilon_\gamma \text{ (= strain invariant)} \quad \ldots\ldots (39)$$

$$\epsilon_{d\alpha\gamma} = \epsilon_\alpha - \epsilon_\gamma \quad \ldots\ldots (40)$$

$$\epsilon_{d\beta\gamma} = \epsilon_\beta - \epsilon_\gamma \quad \ldots\ldots (41)$$

Note that ϵ_α, ϵ_β and ϵ_γ are in general no longer principal strains; rather they are normal strains in the directions of the principal stresses. It may on first thought

seem puzzling that the deviatoric strains $\epsilon_{d\alpha\gamma}$ and $\epsilon_{d\beta\gamma}$ are not necessarily differences between principal strains. This causes however no great problem as the soil model is an incremental one. The total accumulated strains at one instant of time do not necessarily affect the further straining.

Now, the part of the model concerning changes of the principal stresses may be written

$$d[\sigma_m' \; f_s \; bf_s]^T = \mathbf{M} d[\epsilon_v \; \epsilon_{d\alpha\gamma} \; \epsilon_{d\beta\gamma}]^T \quad \ldots\ldots\ldots\ldots \quad (42)$$

or in terms of the principal stress and strain increments

$$d[\sigma_\alpha \; \sigma_\beta \; \sigma_\gamma] = \mathbf{T}_\sigma^{-1} \mathbf{M} \mathbf{T}_\epsilon d[\epsilon_\alpha \; \epsilon_\beta \; \epsilon_\gamma]^T \quad \ldots\ldots\ldots\ldots \quad (43)$$

where $\mathbf{M}$ is still given by Eq. 30 and $\mathbf{T}_\sigma^{-1}$ and $\mathbf{T}_\epsilon$ are given in Appendix.

Finally, rotation of the principal stress directions is governed by

$$d\tau_{ij} = G d\gamma_{ij} \quad \ldots\ldots\ldots\ldots\ldots\ldots\ldots\ldots \quad (44)$$

where i, j = α, β, γ and i $\neq$ j.

The parameter G is a quasi-elastic shear modulus. A discussion on G will follow shortly.

Now, Eqs. 43 and 44 lead to the following incremental relationship:

$$d[\sigma_\alpha \; \sigma_\beta \; \sigma_\gamma \; \tau_{\alpha\beta} \; \tau_{\beta\gamma} \; \tau_{\gamma\alpha}]^T = \mathbf{C} \, d[\epsilon_\alpha \; \epsilon_\beta \; \epsilon_\gamma \; \gamma_{\alpha\beta} \; \gamma_{\beta\gamma} \; \gamma_{\gamma\alpha}]^T \quad . \quad (45)$$

where $\mathbf{C}$ is a 9 by 9 matrix;

$$\mathbf{C} = \begin{bmatrix} \mathbf{T}_\sigma^{-1} \mathbf{M} \mathbf{T}_\epsilon & \mathbf{0} \\ \mathbf{0} & G\mathbf{I} \end{bmatrix} \quad \ldots\ldots\ldots\ldots\ldots\ldots \quad (46)$$

in which $\mathbf{I}$ is a 3 by 3 unit matrix.

In the local axis system α, β, γ all shear stresses vanish. However, for an axis system fixed with respect to derivation, non-vanishing shear stress increments $d\tau_{\alpha\beta}$ etc. may appear along with rotation of the principal stress directions.

Knowing that G is associated with neutral stress changes, it should be fair to hypothesize that this modulus does not depend on the mobilized friction. Requiring also isotropy under hydrostatic stresses one finds the following relation:

$$G = M_{gh} \sin\varphi (\sigma_m' + a) \quad \ldots\ldots\ldots\ldots\ldots\ldots\ldots\ldots \quad (47)$$

where M_{gh} is the value of M_g under hydrostatic stress. When using this relation, no additional test must be run in order to determine G.

However, G may also be determined from tests in which rotation of the principal stress directions takes place. Figure 21 presents the results of three simple shear tests on Model Sand. At the start of shearing, the shear stress imposed is perpendicular to the major principal stress direction. Hence Eq. 44 may be used for interpretation. There is a significant scatter in the test results, partly because of problems with preparing samples with the same density as of the triaxial samples, and partly because of sources of error associated with the small strains appearing at the start of shearing. The laboratory tests result in an average modulus G of 27 MPa, whereas Eq. 47 predicts G = 32 MPa based on the triaxial compression tests. In the opinion of the lecturer the result is encouraging and supporting the adequacy of Eq. 47.

CAPABILITY AND LIMITATIONS OF THE MODEL

A general incremental stress-strain relation was presented above.

The model is defined in a local coordinate system with axes coinciding with the principal stress directions. In order to solve general boundary value problems the model including stresses and strains must be transformed into a global coordinate system. Appropriate transformation rules are given in several textbooks and handbooks, e.g. (22).

Five independent parameters or soil moduli together with the Mohr-Coulomb failure parameters a and φ are included in the model.

Based on available test results, it is believed that each modulus may be determined with reasonable accuracy as a fairly simple function of the mean stress σ_m' and the degree of mobilized friction f_s, or as a function of both. Each modulus may be estimated from different tests. In

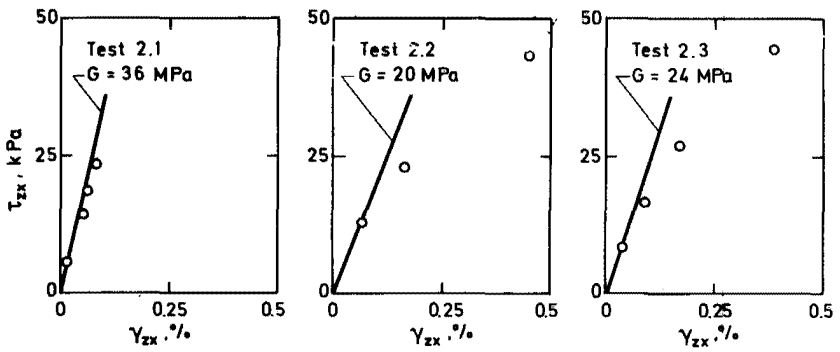

Fig. 21. Results of simple shear tests on Model Sand at the start of shearing under vertical stress $\sigma_z' = 300$ kPa (by the Norwegian Geotechnical Institute).

principle, K_o-triaxial consolidation tests and consolidated undrained triaxial compression tests (CIU) will suffice. However, because of the complexity involved in modelling real soil behaviour in exact terms, it is well advised to determine each modulus as an average result of a number of tests made under stress conditions similar to those of greatest interest. This also goes for the Mohr-Coulomb strength parameters.

The potential of the model itself to describe material behaviour is great. As long as the moduli are carefully determined from appropriate tests, the behaviour predicted by the model is expected to be realistic. However, it is also possible to assign values to the moduli so that the model will describe unrealistic behaviour contradicting the laws of thermodynamics. For instance, if too high value of the dilatancy modulus M_d is applied, the material will expand so as to create work during shearing.

The model can to some extent describe inherent anisotropy, i.e. anisotropy under hydrostatic stresses. It is, however, not designed for this purpose and it is recommended to restrict the moduli to values that exclude inherent anisotropy. This will greatly simplify testing for evaluation of the moduli as well as simplify application of the model. Moreover, the hazard of describing unrealistic behaviour is greatly reduced.

Stress anisotropy is, however, an integral part of the model; appearing soon as stresses deviate from hydrostatic conditions. However, the principal stress directions are always axes of symmetry with respect to the deformation behaviour.

Questions of uniqueness, stability and physical requirements to the moduli have been discussed in some detail in Ref. 32. Presently, a few lines shall be spent on comparison of the model with elasticity and plasticity theories.

As pointed out already, the model was primarily designed to describe soils behaving isotropically under hydrostatic stresses. In order to obtain this, restrictions must be imposed on the values of the shear modulus G and the dilatancy modulus M_d. First, Eq. 47 must be valid, thus relating G to the distortion modulus M_g. Secondly, M_d must be zero. Still considering hydrostatic stresses, the model reduces to

$$d\sigma_m' = M_k d\epsilon_v \quad \ldots\ldots (48)$$

$$d\tau = G d\gamma \quad \ldots\ldots (49)$$

The term quasi-elastic refers to the stress dependency of M_k and G appearing in an incremental stress-strain relation, whereas with the isotropic, linear-elastic behaviour defined in Eqs. 6 and 7 the moduli K and G are constants.

For an isotropic, linear-elastic material, the principal directions of stress and strain always coincide. For the isotropic, quasi-elastic material only the principal directions of the stress and strain increments need coincide. Although Eqs. 48 and 49 defining quasi-elastic behaviour are very similar to Eqs. 6 and 7 defining isotropic, linear-elastic behaviour, it is emphasized that the quasi-elastic behaviour is not truly elastic. For instance, during loading from one stress state to another, the resulting strains do not only depend on the total stress change, as the stress path between the two stress states also matters. Furthermore, during a closed loop of loading the quasi-elastic material does not necessarily recover to the original shape. In spite of these discrepancies it should be fair to consider quasi-elastic behaviour as basically elastic.

Broadly speaking, the soil model presented describes elastic or quasi-elastic behaviour under hydrostatic and near-hydrostatic stresses. As loading takes place under increasing mobilized friction, the distortion modulus M_g, i.e. the resistance to shearing deformation decreases. Yielding or plastic deformation of the soil then gradually takes over. Contrary to elasticity theory, the directions of yield are essentially governed by the directions of the principal stresses rather than by the directions of the increments thereof. Near failure a small increase of the mobilized friction will cause large deformation in the direction of the major principal stress.

As in isotropic, elasto-plastic theory, rotation of the principal stress directions is considered a neutral mode of loading. Rotation of the principal stress directions is governed by the quasi-elastic shear modulus G.

During unloading of an elasto-plastic material, the behaviour is governed by the elastic parameters. This compares well with the behaviour described by the soil model presented when different values of the moduli are used for loading and unloading conditions; the values for unloading conditions reflects the quasi-elastic nature of the soil.

Figure 22 illustrates some of the differences between isotropic, linear-elastic and isotropic, plastic behaviour. The soil model presented may combine both by using proper values of the moduli. The elastic behaviour dominates at near-hydrostatic stresses, during neutral stress changes and unloading, and the plastic behaviour gradually becomes more important as loading towards failure takes place. Although the model is written in terms similar to those of elasticity theory, the resulting behaviour is best compared with elasto-plastic theory.

SUMMARY AND CONCLUSIONS

The first part of the lecture discusses factors affecting soil behaviour. It is emphasized that the effective stress principle is fundamental to soil modelling, and that the Mohr-Coulomb failure criterion is reasonably accurate for soils not inherently anisotropic.

The main goal of this lecture has been to present a new soil behaviour model. The model is defined in terms of mean effective stress, mobilized Mohr-Coulomb fric-

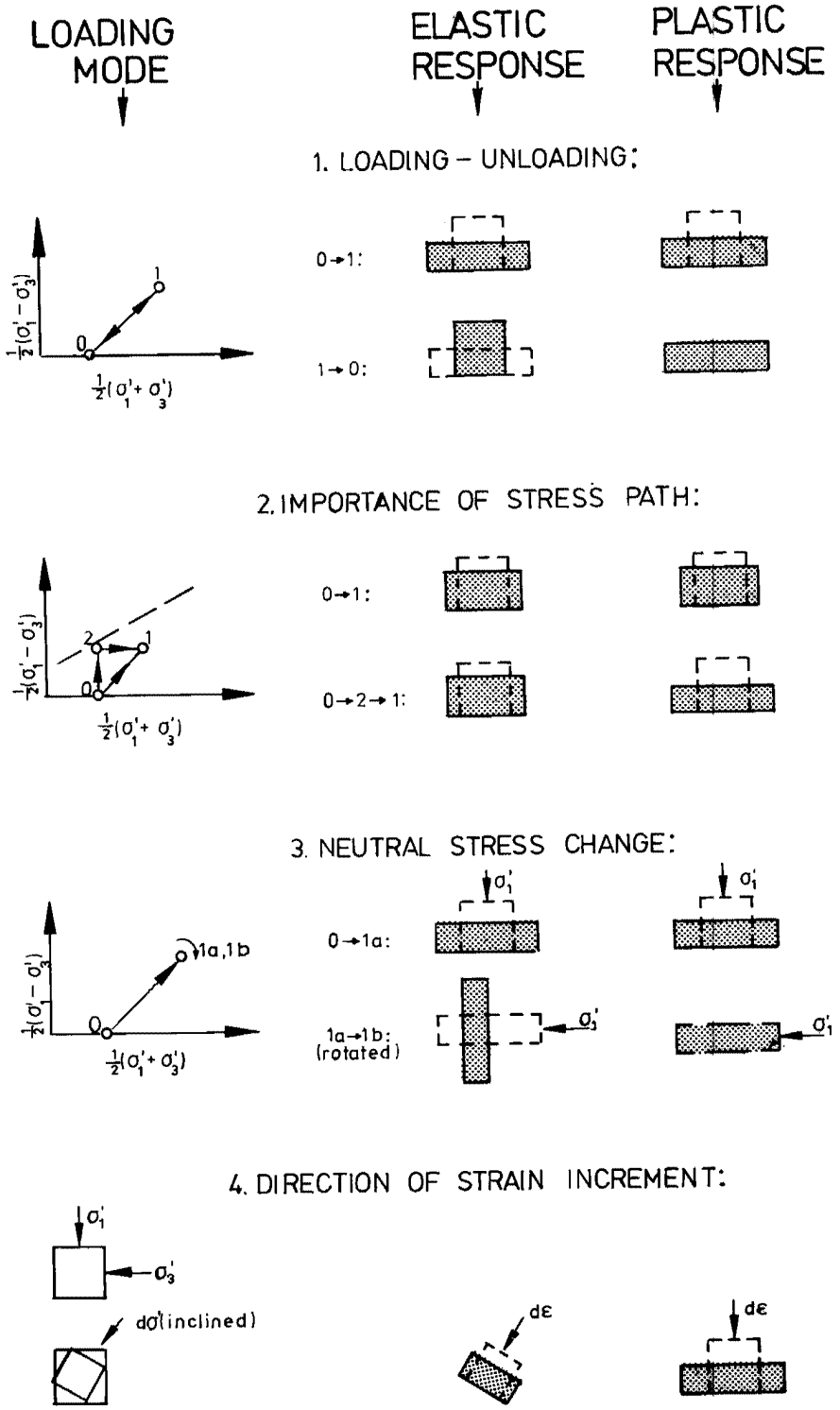

Fig. 22. Examples illustrating deformation behaviour of isotropic, linear-elastic and isotropic, plastic materials under various modes of loading.

tion and volumetric and deviatoric strains. Five independent soil parameters or resistance moduli are included in the model; all of which may be evaluated from conventional triaxial tests.

The model applies to inherently isotropic soil. Stress-induced anisotropy is however accounted for. One of the moduli allows for dilatancy to be dealt with.

The behaviour described by the model is elasto-plastic. Under hydrostatic stresses, the values of the moduli may be chosen so that the behaviour described is isotropic, quasi-elastic. As loading takes place with increasing mobilized Mohr-Coulomb friction, the plastic nature of the behaviour gradually becomes dominant.

The model is general in as far as rotation of the principal stress directions is allowed for; the model is thus applicable for solving of complex boundary value problems.

The asset of the model presented is, in the opinion of the lecturer, the resistance modulus concept. Each of the five moduli has a particular meaning related to the nature of soil behaviour. While some other modulus concepts are too limited in their application, e.g. restricted to fixed principal stress directions, the present model is rather general. Moreover, the plastic nature of soil behaviour is accounted for.

ACKNOWLEDGEMENT

The lecturer is grateful to the Laurits Bjerrum Memorial Fund for the opportunity to give this Lecture, and for the support given.

The lecturer is also indepted to Dr. S. M. Lacasse and Dr. K. Høeg for critisism and valuable comments during preparation of the manuscript.

REFERENCES

1. Aas, G. (1976): *Totalspenningsanalyser, prinsipp, grunnlag. Stabilitetsberegning for fylling på kvikkleire, Elllingsrud, Oslo. Bæreevneberegning for direkte fundamentert silo ved Moss aktiemøller. Vurdering av en 10 m dyp åpen utgravning for postgiro- og jernbanehuset i Oslo. Stabilitetsberegning for vel 10 m dyp avstivet utgravning for postgiro- og jernbaneposthuset i Oslo.* (Five papers in Norwegian). Norske sivilingeniørers forening. Jordartsegenskaper, bestemmelse og anvendelse ved stabilitetsanalyser i leire. (Soil properties; their estimation and application in stability analyses of clay). Kurs Gol 1976.
2. Berre, T. and L. Bjerrum (1973): *Shear strength of normally consolidated clays.* International Conference on Soil Mechanics and Foundation Engineering, 8. Moscow 1973. Proceedings, Vol. 1.1, pp. 39–49. Also publ. in: Norwegian Geotechnical Institute. Publication, 99.
3. Bishop, A.W. and L.D. Wesley (1975): *A hydraulic triaxial apparatus for controlled stress path testing.* Géotechnique, Vol. 25, No. 4, pp. 657–670.
4. Bjerrum, L. (1973): *Problems of soil mechanics and construction on soft clays.* State-of-the-art report to session IV. International Conference on Soil Mechanics and Foundation Engineering, 8. Moscow 1973. Proceedings, Vol. 3, pp. 111–159. Also publ. in: Norwegian Geotechnical Institute. Publication, 100.
5. Campanella, R.G. (1973): *Influence of stress path on the plane strain behaviour of a sensitive clay.* International Conference on Soil Mechanics and Foundation Engineering, 8. Moscow 1973. Proceedings, Vol. 1.1, pp. 85–92.
6. Clough, R.W. and R.J. Woodward, III. (1967): *Analyses of embankment stresses and deformations.* American Society of Civil Engineers. Proceedings, Vol. 93, No. SM 4, pp. 529–549.
7. Drucker, D.C. and W. Prager (1952): *Soil mechanics and plastic analysis or limit design.* Quarterly of Applied Mathematics, Vol. 10, No. 2, pp. 157–165.
8. Drucker, D.C. (1953): *Limit analysis of two- and three-dimensional soil mechanics problems.* Journal of the Mechanics and Physics of Solids, Vol. 1, pp. 217–226.
9. Duncan, J.M. and C.-Y. Chang (1970): *Nonlinear analysis of stress and strain in soils.* American Society of Civil Engineers. Proceedings, Vol. 96, No. SM 5, pp. 1629–1653.
10. Girijavallabhan, C.V. and L.C. Reese (1968): *Finite-element method for problems in soil mechanics.* American Society of Civil Engineers. Proceedings, Vol. 94, No. SM 2, pp. 473–496.
11. Green, G.E. (1972): *Strength and deformation of sand measured in an independent stress control cell.* Roscoe Memorial Symposium. Cambridge University 1971. Proceedings. Stress-strain behaviour of soils. Ed. by R.H.G. Parry. Pp. 285–323.
12. Høeg, K. (1978): *Deformation computations in geotechnical engineering.* The Second Laurits Bjerrum Lecture presented 14th March 1977. Norwegian Geotechnical Institute. Publication, 123. 19 p.
13. International Conference on Soil Mechanics and Foundation Engineering, 9. Tokyo 1977 (1978). Specialty session, 9: Constitutive equations. Ed. by S. Murayama and A.N. Schofield. Tokyo 1978. 310 p.
14. Janbu, N. (1963): *Soil compressibility as determined by oedometer and triaxial tests.* European Conference on Soil Mechanics and Foundation Engineering. Wiesbaden 1963. Proceedings, Vol. 1, pp. 19–25.
15. Janbu, N. (1973): *Shear strength and stability of soils; the applicability of the Coulombian material 200 years after the ESSAI.* Norsk geoteknisk forening. NGF-foredraget 1973. Oslo, Norwegian Geotechnical Institute. 47 p.
16. Ko, H.-Y. and R.F. Scott (1968): *Deformation of sand at failure.* American Society of Civil Engineers. Proceedings, Vol. 94, No. SM 4, pp. 883–898.
17. Ladd, C.C. and R. Foot (1974): *New design procedure for stability of soft clays.* American Society of Civil Engineers. Proceedings, Vol. 100, No. GT 7, pp. 763–786.
18. Lade, P.V. and J.M. Duncan (1973): *Cubical triaxial tests on cohesionless soil.* American Society of Civil Engineers. Proceedings, Vol. 99, No. SM 10, pp. 793–812.
19. Lade, P.V. and J.M. Duncan (1975): *Elastoplastic stress-strain theory for cohesionless soil.* American Society of Civil Engineers. Proceedings, Vol. 101, No. GT 10, pp. 1037–1053.
20. Lambe, T.W. (1964): *Methods of estimating settlement.* American Society of Civil Engineers. Proceedings, Vol. 90, No. SM 5, pp. 43–67.
21. Masson, R.M. (1971): *Nonlinear characterization and stress analysis in a granular material.* Ph.D. Dissertation. University of Colorado, Boulder.
22. Poulos, H. and Davis, E.H. (1974): *Elastic solutions for soil and rock mechanics.* New York, Wiley. 411 p.
23. Prévost, J.-H. and K. Høeg (1975): *Effective stress-strain-strength model for soils.* American Society of Civil Engineers. Proceedings, Vol. 101, No. GT 3, pp. 259–278. Also publ. in: Norwegian Geotechnical Institute. Publication, 107.

24. Prévost, J.-H. and K. Høeg (1977): *Plasticity model for undrained stress-strain behavior.* International Conference on Soil Mechanics and Foundation Engineering, 9. Tokyo 1977. Proceedings, Vol. 1, pp. 255–261. Also publ. in: Norwegian Geotechnical Institute. Publication, 118.
25. Roscoe, K.H. and A.N. Schofield (1963): *Mechanical behaviour of an idealised 'Wet-Clay'.* European Conference on Soil Mechanics and Foundation Engineering, 3. Wiesbaden 1963. Proceedings, Vol. 1, pp. 47–54.
26. Roscoe, K.H., A.N. Schofield and A. Thurairajah (1963): *Yielding of clays in states wetter than critical.* Géotechnique, Vol. 13, No. 3, pp. 211–240.
27. Schofield, A. and P. Wroth (1968): *Critical state soil mechanics.* New York, McGraw-Hill. 310 p.
28. Shibata, T. and D. Karube (1965): *Influence of the variation of the intermediate principal stress on the mechanical properties of normally consolidated clays.* International Conference on Soil Mechanics and Foundation Engineering, 6. Montreal 1865. Proceedings, Vol. 1, pp. 359–363.
29. Sutherland, H.B. and M.S. Mesdary (1969): *The influence of the intermediate principal stress on the strength of sand.* International Conference on Soil Mechanics and Foundation Engineering, 7. Mexico 1969. Proceedings, Vol. 1, pp. 391–399.
30. Terzaghi, K. (1936): *The shearing resistance of saturated soils and the angle between the planes of shear.* International Conference on Soil Mechanics and Foundation Engineering, 1. Cambridge, Mass. 1936. Proceedings, Vol. 1, pp. 54–56.
31. Terzaghi, K. (1960): *From theory to practice in soil mechanics.* Selections from the writings of Karl Terzaghi. New York, Wiley. 425 p.
32. Tokheim, O. (1976): *A model for soil behaviour.* Dissertation submitted for the Dr. techn. degree. The Norwegian Institute of Technology, Trondheim. Soil Mechanics and Foundation Engineering. 215 p.
33. Wong, P.K.K. and R.J. Mitchell (1975): *Yielding and plastic flow of sensitive cemented clay.* Géotechnique, Vol. 25, No. 4, pp. 763–782.
34. Zienkiewicz, O.C., C. Humpheson and R.W. Lewis (1975): *Associated and non-associated visco-plasticity and plasticity in soil mechanics.* Géotechnique, Vol. 25, No. 4, pp. 671–689.

Appendix

TRANSFORMATION OF STRESS AND STRAIN INCREMENTS

Equations 4, 5 and 27, relating volumetric and deviatoric strains to principal strains, may be rephraced as follows:

$$[\epsilon_v\ \epsilon_{d13}\ \epsilon_{d23}]^T = \mathbf{T}_\epsilon[\epsilon_1\ \epsilon_2\ \epsilon_3]^T \quad \text{(A-1)}$$

in which

$$\mathbf{T}_\epsilon = \begin{bmatrix} 1 & 1 & 1 \\ 1 & 0 & -1 \\ 0 & 1 & -1 \end{bmatrix} \quad \text{(A-2)}$$

Equation (A-1) is valid for strain increments also, hence

$$d[\epsilon_v\ \epsilon_{d13}\ \epsilon_{d23}]^T = \mathbf{T}_\epsilon\, d[\epsilon_1\ \epsilon_2\ \epsilon_3]^T \quad \text{(A-3)}$$

The following relationship holds between increments of stress functions and increments of principal stresses:

$$d[\sigma_m'\ f_s\ bf_s]^T = \mathbf{T}_\sigma d[\sigma_1'\ \sigma_2'\ \sigma_3']^T \quad \text{(A-4)}$$

Still, σ_m' is the mean effective stress, f_s is the degree of mobilized friction (Mohr-Coulomb) defined in Eq. 11 and b is the relative magnitude of the intermediate principal stress defined in Eq. 26.

The matrix $\mathbf{T}_\sigma$ is given by

$$\mathbf{T}_\sigma = \frac{1}{6\sigma_s'\sin\varphi} \begin{bmatrix} 2\sigma_s'\sin\varphi & 2\sigma_s'\sin\varphi & 2\sigma_s'\sin\varphi \\ 3(1-f_s\sin\varphi) & 0 & -3(1+f_s\sin\varphi) \\ -3bf_s\sin\varphi & 3 & -3(1+bf_s\sin\varphi) \end{bmatrix} \quad \text{(A-5)}$$

in which the following abbreviation is used:

$$\sigma_s' = \tfrac{1}{2}(\sigma_1' + \sigma_3') + a \quad \text{(A-6)}$$

or in terms of stress functions

$$\sigma_s' = \frac{3(\sigma_m' + a)}{3-(1-2b)f_s\sin\varphi} \quad \text{(A-7)}$$

When inserting Eqs. (A-3) and (A-4) into Eq. 29, Eq. 31 is arrived at. In the latter equation, which is a relation between increments of principal stresses and strains, $\mathbf{T}_\sigma^{-1}$ is the inverse of $\mathbf{T}_\sigma$;

$$\mathbf{T}_\sigma^{-1} = \frac{1}{3-(1-2b)f_s\sin\varphi} \begin{bmatrix} 3(1+f_s\sin\varphi) & 2(2+bf_s\sin\varphi)\sigma_s'\sin\varphi & -2(1+f_s\sin\varphi)\sigma_s'\sin\varphi \\ 3[1-(1-2b)f_s\sin\varphi] & -2\sigma_s'\sin\varphi & 4\sigma_s'\sin\varphi \\ 3(1-f_s\sin\varphi) & -2(1+bf_s\sin\varphi)\sigma_s'\sin\varphi & -2(1-f_s\sin\varphi)\sigma_s'\sin\varphi \end{bmatrix} \quad \text{(A-8)}$$

So far, coinciding, fixed principal stress and strain directions have been considered. In a general case not restricted to a particular type of loading, the principal directions of stresses and strains and increments thereof need not coincide. However, in Ref. 32 it is argued that all equations given above are still valid when the labels 1, 2 and 3 are substituted with α, β and γ denoting the current principal *stress* directions. Hence Eq. 43 is arrived at.